Numerical Study of Dense Turbulent Sprays using a Coupling of the Direct Quadrature Method of Moments with an Eulerian Multi-Size Moment Model

W. Gumprich*, A. Sadiki
Institute of Energy and Powerplant Technology,
Graduate School of Computational Engineering,
Technische Universität Darmstadt, Germany
gumprich@ekt.tu-darmstadt.de and sadiki@ekt.tu-darmstadt.de

Abstract

This contribution aims at including droplet-droplet interactions into an Eulerian framework using the Direct Quadrature based Sectional Method of Moments (DQbSMOM), a novel hybrid approach which combines the Direct Quadrature Method of Moments (DQMOM), proposed by Fox et al. [1], with a Sectional Method (SM). This is made possible by approximating the number density function (NDF) through the Maximal Entropy formalism in order to calculate the droplet coalescence term, and by adopting the Eulerian Multi-Size Moment model (EMSM), proposed by Massot et al. [2], to describe evaporating droplet polydispersity. The EMSM model provides not only an accurate prediction of the evaporative flux, but also the possibility to couple DQMOM with a SM, once the moment flux between two sections can be calculated. The major advantage of this hybrid approach is a higher accuracy related to convective transport and drag. Among the advantages of the Eulerian approach are a lower computational cost through optimal parallel computing and a straightforward liquid-gas phase coupling. To assess the designed tool, numerical results are compared to Phase Doppler Anemometry (PDA) measurements of a hollow-cone water spray as experimentally investigated by Rüger et al. [3]. The experiment provides comprehensive validation data that include gas velocities, droplet size distribution and droplet velocities. Turbulence is captured by two different k-ϵ based models. Satisfactory agreement is observed with increasing number of sections, allowing a better description of polydispersity.

Introduction

The polydisperse spray character of the injected liquid fuel predominantly influences the mixing of oxidizer and fuel vapour and, consequently, the flame structure in combustion processes, considerably affecting combustion efficiency and emissions in IC-engines and gas turbines. Especially due to increasing fuel prices and stronger emissions regulations, there is a need for a reliable numerical tool to accurately describe and optimize the dense spray behavior in modern engines.

On a mesoscopic level, there are two main approaches for the spray modeling: the Euler-Lagrange (EL) and the Euler-Euler (EE) methods. Both are based on a mesoscopic description relying on a kinetic Boltzmann type equation known as the Williams spray equation [4]. The EL method, also known as the Direct Simulation Monte-Carlo method (DSMC), is able to describe the complexity of occurring physical phenomena in a straightforward way, once the simulated particles (*parcels*) are *tracked* individually with a Lagrangian approach. Although the EL method is generally considered the most robust, reliable and accurate approach for the spray simulation, its computational cost strongly depends on the unsteadiness of the flow and mass loading of the system [5]. In order to avoid a high level of statistical noise and achieve an accurate and smooth continuous field of the droplet averaged properties, a sufficient amount of sampled parcels is required. This necessary amount of parcels increases considerably when unsteady simulations, that require fine time and spatial discretizations, are performed. Especially in the case of Large Eddy Simulation (LES), the necessary amount of sampled parcels per time step and grid cell is considerably higher in comparison to RANS models, since LES is less dissipative than RANS. Nevertheless, a RANS-approach is followed in this paper. Also among the drawbacks of EL models is the difficulty in the accurate coupling between the Lagrangian disperse phase and the Eulerian continuous phase, and in achieving an optimal parallelization of the solver, since most parcels are located in a small region of the computational domain.

A promising alternative to EL methods is the EE approach. Also known as Eulerian moment methods, EE models calculate the evolution of the moments of the number density function (NDF) with a set of Navier-Stokes-like transport equations. The structure of these equations and their computational cost does not depend on the droplet mass load or the unsteadiness of the system. Since the equations of both disperse and continuous phase share the

*Corresponding author: gumprich@ekt.tu-darmstadt.de

same structure, the coupling between both phases is straightforward and solver parallelization can be optimized. For these reasons, there is a growing interest in the development of reliable Eulerian moment models for the spray simulation. Several approaches and their variations are found in the literature, such as the Quadrature Method of Moments (QMOM) [6], the Direct Quadrature Method of Moments (DQMOM) [1] and the class or Sectional Methods (SM) [2, 7, 18], each of them with their advantages and drawbacks. In the case of DQMOM, a major challenge involves the accurate description of convective transport and drag effects. The general DQMOM approach is to approximate the NDF by a few quadrature points and assume that all droplets of a certain size locally share the same velocity (mono-kinetic assumption), such that, regarding convective transport and drag, these quadrature points are handled as ordinary disperse phases of a multi-fluid model. Therefore, in its standard form, DQMOM is not suitable for the simulation of spray systems involving high droplet-gas relative velocities. A similar issue has been recently tackled by Vié et al. [14], who proposed a new model called Coupled Size-Velocity Moments (CSVM) model, within a moment method framework. The CSVM model addresses size-velocity correlations in drag and convectional transport processes.

In this work, a novel hybrid approach, referred to as the Direct Quadrature based Sectional Method of Moments (DQbSMOM), which combines DQMOM with a SM, is proposed. The idea is to split the droplet size space into sections, as in a SM, and to approximate the NDF with weighted Dirac-delta functions over each section. Following an operator splitting method, droplet coalescence and evaporation are handled separately from the multi-fluid system. A new approach for calculating droplet coalescence, based on the reconstruction of the NDF through a Maximal Entropy formalism is proposed, while the droplet evaporation is calculated according to the Eulerian Multi-Size Moment (EMSM) model, proposed by Massot et al. [2]. The simple d^2-law of evaporation is first used. Two k-ϵ based turbulence models for the disperse phase, namely the Simonin & Viollet and Chesters & Issa model, are applied to retrieve the influence of turbulence modeling of the disperse phase within the RANS framework.

Numerical Method

The Direct Quadrature based Sectional Method of Moments

The spray is characterized by the joint number density function $f(v, \mathbf{u}; \mathbf{x}, t)$ of droplet volume and velocity. The evolution of $f(v, \mathbf{u}; \mathbf{x}, t)$ is described by a kinetic Boltzmann type equation proposed by Williams [4]:

$$\partial_t f + u_i \partial_{x_i} f + \partial_v (R_v f) + \partial_{u_i} (F_i f) = \Gamma, \tag{1}$$

where R_v describes the evaporation rate, F_i are the forces acting on the droplet (i.e. drag), and Γ is the droplet coalescence term, derived from the kinetic theory of gases.

In an Eulerian framework, the Williams equation is solved using the DQbSMOM, a novel hybrid approach which combines the Direct Quadrature Method of Moments (DQMOM), introduced by Marchisio and Fox [8], with a Sectional Method (SM) [2, 7, 18]. Thus, the droplet size space is divided into intervals (also called sections) and the NDF is approximated by weighted Dirac-delta functions over each section k:

$$f^k(v, \mathbf{u}) \approx \sum_{n=1}^{N} w_n^k \delta(v - v_n^k) \delta(\mathbf{u} - \mathbf{u}_n^k) \tag{2}$$

After inserting the approximation (2) into the Williams equation (1), transport equations for the number density, mass density and momentum density are derived [1]:

$$\partial_t (w_n^k) + \partial_{x_i} (w_n^k u_{i,n}^k) = a_n^k \tag{3}$$

$$\partial_t (\rho w_n^k v_n^k) + \partial_{x_i} (\rho w_n^k v_n^k u_{i,n}^k) = \rho b_n^k \tag{4}$$

$$\partial_t (\rho w_n^k v_n^k u_{j,n}^k) + \partial_{x_i} (\rho w_n^k v_n^k u_{j,n}^k u_{i,n}^k) = \rho c_{j,n}^k \tag{5}$$

Closure for the terms a_n^k, b_n^k and $c_{j,n}^k$, on the right hand side of equations (3), (4) and (5), is generally achieved by applying moment transforms to both sides of the Williams equation:

$$\int v^q u_1^l u_2^m u_3^p (\partial_t f + u_i \partial_{x_i} f) dv d\mathbf{u} = \int v^q u_1^l u_2^m u_3^p (\Gamma - \partial_v (R_v f) - \partial_{u_i} (F_i f)) dv d\mathbf{u} \tag{6}$$

Then, a linear system of equations is derived from equation (6) after a choice of $5N$ moments. The terms a_n^k, b_n^k and $c_{j,n}^k$ are generally determined by *solving* this linear system (see [1]). However, this procedure does not exactly apply to all physical effects considered, which are handled separately as described in the following subsections.

Coupling to a Multi-Fluid Method

Following a mono-kinetic assumption, only moments of order 0 and 1 are considered for the velocity components, such that all terms accounting for the forces acting on the droplets are de-coupled from the DQMOM system (6). Then, the DQMOM is coupled to a multi-fluid method by considering each abscissa n of each section k to represent a disperse phase in the multi-fluid system, and by defining the phase volume fraction as $\alpha_n^k = w_n^k v_n^k$, where w_n^k is the number of droplets per volume unit. Hence, the left hand side (LHS) of equations (4) and (5) are equal to the LHS of the continuity and momentum transport equations of a multi-fluid method, respectively:

$$\partial_t(\rho w_n^k v_n^k) + \partial_{x_i}(\rho w_n^k v_n^k u_{i,n}^k) = \quad \partial_t(\rho \alpha_n^k) + \partial_{x_i}(\rho \alpha_n^k u_{i,n}^k) \quad = 0 \tag{7}$$

$$\partial_t(\rho w_n^k v_n^k u_{j,n}^k) + \partial_{x_i}(\rho w_n^k v_n^k u_{j,n}^k u_{i,n}^k) = \quad \partial_t(\rho \alpha_n^k u_{j,n}^k) + \partial_{x_i}(\rho \alpha_n^k u_{j,n}^k u_{i,n}^k) \quad = RHS \tag{8}$$

Additionally to the drag term, the RHS of equation (8) also includes turbulence diffusion and gravity effects. Regarding turbulence, the mathematical correctness of this coupling approach has been addressed by Belt and Simonin [9]. Satisfactory results have been achieved by different authors (see [10, 11, 12]) by following this coupling method.

Turbulence is modeled with the standard k-ϵ model. k and ϵ equations, extended to account for interphase interaction terms, are solved for the continuous phase only. The turbulence of the disperse phase is modeled according to approaches of Simonin & Viollet [13, 15] and Chesters & Issa (see in [16]), respectively. In both cases, a double averaging approach is followed. That is, after a volume average, a Favre average is applied to the transport equations of each phase. The advantage of this double averaging approach is that no additional terms are present in the averaged continuity equations.

According to Simonin & Viollet [15], turbulence quantities of the disperse phase can be determined in terms of the mean characteristics of the continuous phase and the ratio of droplet relaxation and eddy-droplet interaction times. The turbulent kinetic energy of the disperse phase is given by:

$$k_d \quad = \quad \left(\frac{b^2+\eta}{1+\eta}\right) k_c \tag{9}$$

where η is the ratio between the time of correlated turbulent motion and the droplet relaxation time, and b depends on the coefficient of added mass and on the ratio between the liquid and gas densities.

Following the approach proposed by Politis [17], Chesters & Issa consider a response coefficient C_t to relate the turbulent kinetic energy of the disperse phase to the one of the continuous phase:

$$k_d \quad = \quad C_t^2 \, k_c \tag{10}$$

with

$$C_t = \frac{3+\beta}{1+\beta+2\rho_d/\rho_c} \quad \text{and} \quad \beta = \frac{12 A_d}{\pi d \mu}\left(\frac{l_e}{d}\right)\frac{1}{Re_t}, \tag{11}$$

where l_e is the turbulence length scale, μ describes the gas viscosity and Re_t is the turbulence Reynolds number. The friction coefficient A_d depends on the drag coefficient, droplet diameter d and droplet-gas relative velocity. The densities of the disperse and continuous phases are described by ρ_d and ρ_c, respectively. Moreover, the influence of turbulence on droplet drag is taken into account by both models. For detailed information on the modeling of turbulence stress and drag, please refer to the referenced literature.

Operator Splitting

The occurring physical phenomena are handled separately by considering an operator splitting approach (see [18]). More precisely, droplet coalescence and droplet evaporation are computed individually and separately from the multi-fluid system, such that the Williams equation (1) is split into the following system:

$$\partial_t f + u_i \partial_{x_i} f \quad = \quad -\partial_{u_i}(F_i f) \tag{12}$$

$$\partial_t f \quad = \quad -\partial_v(R_v f) \tag{13}$$

$$\partial_t f \quad = \quad \Gamma \tag{14}$$

The solution of the full problem is approximated by alternatively solving equations (12), (13) and (14). It is interesting to notice that applying DQMOM to the equation (12) results in the multi-fluid system composed by equations (3), (7) and (8), with $a_n^k = 0$.

Droplet Coalescence

The droplet coalescence term can be separated into two parts: $\Gamma = Q^-_{coll} + Q^+_{coll}$, which account for the droplets killed and created, respectively [1]:

$$Q^-_{coll}(v) = -\int\int_0^\infty B(|\mathbf{u}-\mathbf{u}'|, v, v')f(v,\mathbf{u})f(v',\mathbf{u}')dv'd\mathbf{u}', \quad (15)$$

$$Q^+_{coll}(v) = \frac{1}{2}\int\int_0^v B(|\mathbf{u}^o-\mathbf{u}'|, v^o, v')f(v^o,\mathbf{u}^o)f(v',\mathbf{u}')Jdv'd\mathbf{u}', \quad (16)$$

where $v^o = v - v'$, $\mathbf{u}^o = (v\mathbf{u} - v'\mathbf{u}')/(v-v')$, and $J = (v/v^o)^3$ is the Jacobian of the transform $(v,\mathbf{u}) \rightarrow (v^o,\mathbf{u}^o)$ with fixed $(v',\mathbf{u})'$. B is the collision frequency defined by

$$B(|\mathbf{u}^o-\mathbf{u}'|, v^o, v') = \pi\left(\frac{d^o}{2}+\frac{d'}{2}\right)^2|\mathbf{u}^o-\mathbf{u}'|, \;\; d = \left(\frac{6}{\pi}v\right)^{(1/3)} \quad (17)$$

Then, similarly to the standard DQMOM approach proposed by Fox et al. [1], moment transforms (6) are applied to both sides of equation (14), and a linear system is derived after a choice of $5N$ moments. The LHS of this linear system is given by:

$$\int\int_{v_{k-1}}^{v_k} v^q u_1^l u_2^m u_3^p(\partial_t f)dvd\mathbf{u} = \sum_{n=1}^N (1-q)(v_n^k)^q(\mathbf{u}_n^k)^{lmp}a_n^k + \quad (18)$$

$$\sum_{n=1}^N (q-l-m-p)(v_n^k)^{q-1}(\mathbf{u}_n^k)^{lmp}b_n^k + \sum_{n=1}^N (v_n^k)^{q-1}(\mathbf{u}_n^k)^{lmp}[lc_{1,n}^k/u_{1,n}^k + mc_{2,n}^k/u_{2,n}^k + pc_{3,n}^k/u_{3,n}^k]$$

with $(\mathbf{u}_n^k)^{lmp} = (u_{1,n}^k)^l(u_{2,n}^k)^m(u_{3,n}^k)^p$. Note that the moment transforms are integrated over each section k ($v \in [v_{k-1}, v_k]$). Hence, the NDF must be priorly known in order to numerically integrate the RHS of the system:

$$\int\int_{v_{k-1}}^{v_k} v^q u_1^l u_2^m u_3^p(Q^-_{coll}(v) + Q^+_{coll}(v))dvd\mathbf{u} = Q^-_{k,qlmp} + Q^+_{k,qlmp} \quad (19)$$

The NDF is approximated from its moments by Entropy Maximization (see [2, 19]). The velocity as a function of droplet size is approximated using the strategy proposed by Vié et al. [14]. A two-dimensional Newton-Cotes quadrature is used to numerically integrate the coalescence term. It is also interesting to mention that the integration nodes are fix for all sections S_i with $i \in [1, N_{sec}-1]$, N_{sec} is the number of sections, such that the total amount of operations as well as the computational cost of the model are significantly reduced. For more information, please consult the referenced literature.

Evaporation

Droplet evaporation is calculated with the Eulerian Multi-Size Moment (EMSM) model, proposed by Massot et al. [2], considering the simple d^2-law of evaporation:

$$\frac{d(d^2)}{dt} = R_s(t) \quad (20)$$

where $R_s(t)$ describes the evaporation rate. In this case, the EMSM model considers that, over a small time-step Δt, the NDF of droplet surface $f(s)$ is simply shifted over the s-axis without changing its shape. The length of this shift is equal to $R_s(t)\Delta t$. The moment flux between the section boundaries as well as the droplet evaporative flux are predicted by integrating a reconstruction of $f(s)$ over each boundary shift. This reconstruction is achieved through the Maximal Entropy formalism. For a detailed description of the model, please see [2, 18]. In principle, the EMSM algorithm can be extended to advanced evaporation models [22, 23].

Experimental and Numerical Configuration

The experimental configuration considered for the assessment of the implemented numerical model concerns a water hollow-cone spray under ambient conditions (20.9°C air temperature). Although droplet evaporation is not neglectable, the configuration was designed for validating results regarding spray evolution and droplet coalescence effects. Phase Doppler Anemometry (PDA) measurements were conducted by Rüger et al. [3] at four positions

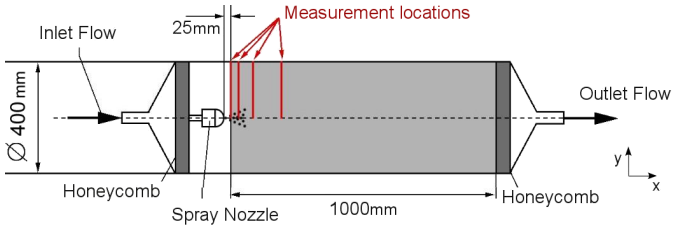

Figure 1. Experimental geometry [3].

located from 25mm to 200mm downstream of the nozzle, as illustrated in figure 1. The occurrence of secondary droplet breakup is neglectable after the first measurement location. For additional information, the reader may refer to [3].

The inlet of the simulation domain is located at the first measurement location (x=25mm) and the measured data were considered as boundary conditions. DQMOM quadrature points over the inlet profile were calculated using the Product Difference algorithm (see [10, 21]). Transient simulations were performed using a structured 3D mesh with 640,000 cells and considering a time-step of 7.5e-5 seconds. In the near nozzle region, the cells have a length of about 1mm in each coordinate direction. A mesh dependency study has been previously performed. Unsteady calculations were conducted until a stationary state was reached.

Results and Discussion

In order to illustrate the accuracy of the DQbSMOM hybrid approach concerning convectional transport and drag, four simulations with a different amount of sections were performed. The first one is a regular DQMOM approach, with only one section and 3 quadrature points. The others consider 3, 4 and 5 sections, respectively, and 2 quadrature points per section. The results were achieved with and without considering droplet coalescence and evaporation processes. Droplet coalescence and evaporation are not first considered with the aim of isolating convectional transport and drag effects. However, it is interesting to mention that the influence of droplet coales-

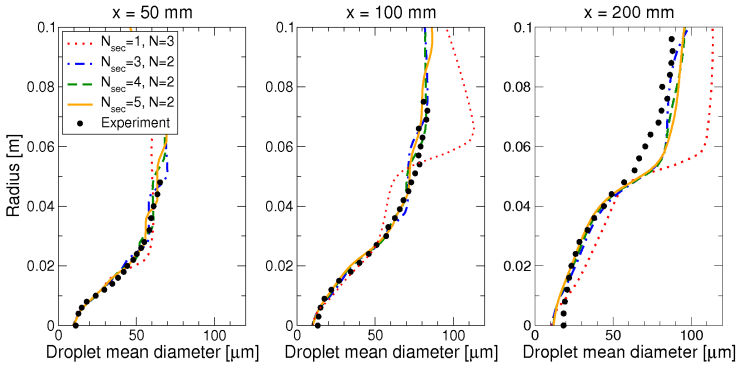

Figure 2. Droplet mean diameter over different measurement profiles.

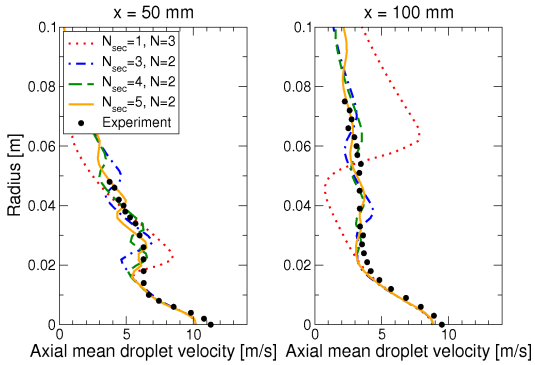

Figure 3. Axial mean droplet velocity.

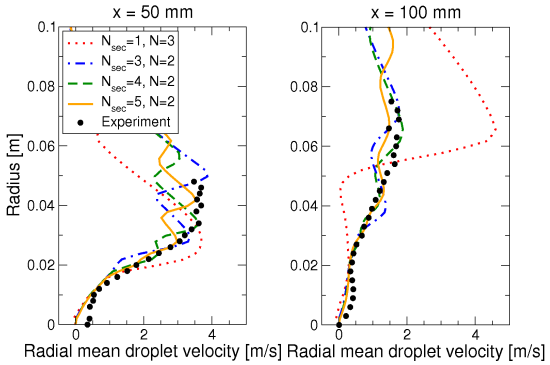

Figure 4. Radial mean droplet velocity.

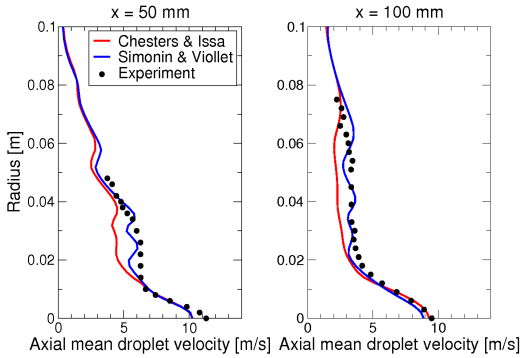

Figure 5. Axial mean droplet velocity.

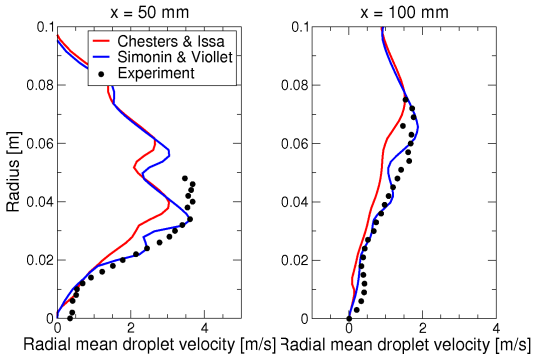

Figure 6. Radial mean droplet velocity.

cence and evaporation on the radial profiles of the droplet mean properties is little. Results are provided in figures 2, 3 and 4, where profiles of mean droplet diameter and droplet mean axial and radial velocities are plotted over different measurement locations. The zig-zag pattern of these profiles are errors associated to droplet dispersion, majorly influenced by convectional transport and drag. One can see that this error is substantial if only one section is considered. As the amount of sections is increased, the deviation from experimental results is considerably reduced. The reason for that is not only an increase in the total amount of quadrature points, but also the choice of these points. While the choice of DQMOM points over a section depends only on the Product Difference algorithm, the sections were determined in such a way that the integral droplet mass is more or less equally distributed over the sections at the inlet location. The results in figures 2, 3 and 4 were calculated using the Simonin & Viollet approach for modeling the turbulence of the disperse phase.

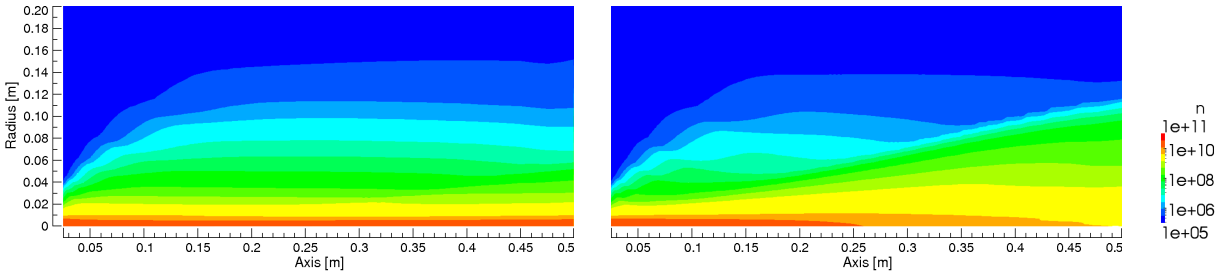

Figure 7. Droplet number concentration calculated using the Chesters & Issa (left) and the Simonin & Viollet (right) turbulence models, without droplet coalescence.

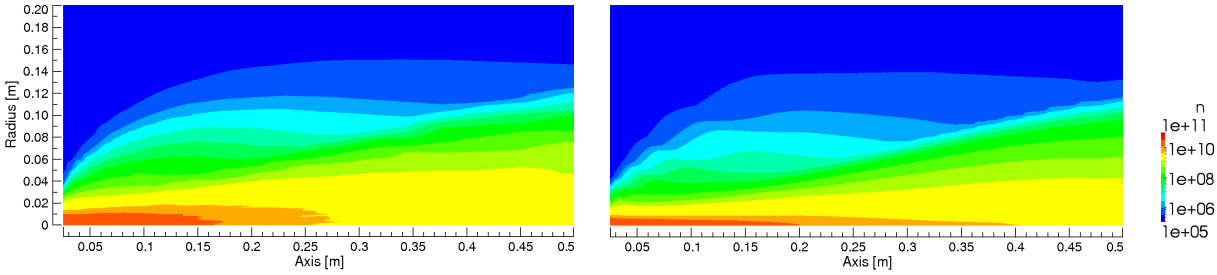

Figure 8. Droplet number concentration from experimental measurements (left) and simulation using the Simonin & Viollet turbulence model including droplet coalescence (right).

Although the DQbSMOM considerably increases the accuracy related to droplet dispersion, the turbulence modeling also plays a significant role. For this reason, two different approaches for modeling the turbulence of the disperse phase are evaluated: Simonin & Viollet [15] and Chesters & Issa (see in [16]). One can see in figures 5 and 6 that the results delivered by the Simonin & Viollet model are considerably more accurate. It is also interesting to notice that the Chesters & Issa model achieves smoother curves. Qualitatively, the higher accuracy of the Simonin & Viollet model can be noticed in figures 7 and 8, where contours of droplet concentration are plotted. In comparison to the experimental data (figure 8, left), the model of Simonin & Viollet (figure 7, right) is able to qualitatively predict radial droplet dispersion in the dense spray region with a satisfactory accuracy. Similar

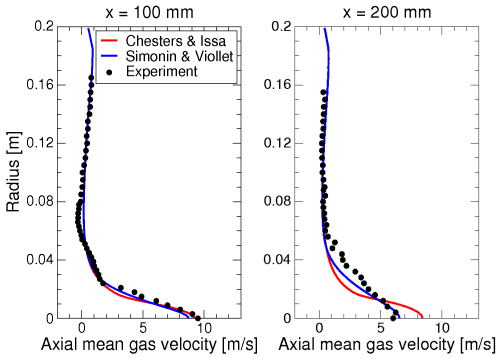

Figure 9. Axial mean gas velocity.

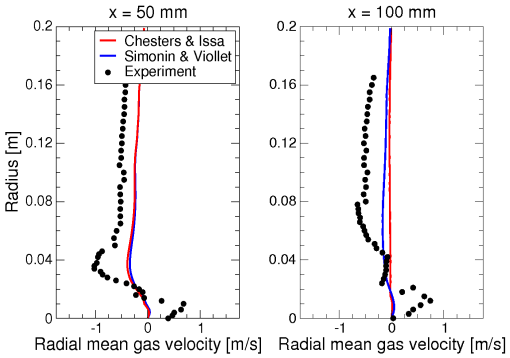

Figure 10. Radial mean gas velocity.

to experimental measurements, the spray angle can be clearly noticed. In contrast, Chesters & Issa poorly predicts radial droplet dispersion, especially after a distance of about 0.1m from the nozzle, such that the contours are nearly flat along the spray axis and a spray angle is not noticeable. In addition, the standard k-ϵ model itself is unable to accurately predict the radial mean gas velocity (see figure 10), negatively influencing radial droplet dispersion. Farther from the nozzle, the Chesters & Issa model increases even more the already high error associated to the k-ϵ model. However, the axial mean gas velocity is predicted with a reasonable accuracy by the k-ϵ model, as seen in figure 9, and the Simonin & Viollet model does not affect this trend. Simulations were performed considering the case with 4 sections.

Under consideration of droplet coalescence and evaporation, the results obtained are displayed in figures 8, 11 and 12. Qualitatively, the importance of droplet coalescence can be noticed by comparing figures 7 (right) and 8 (right) to experimental measurements illustrated in figure 8 (left). The calculations concern the same simulation case, that is, the case with 4 sections, 2 quadrature points per section, and using the Simonin & Viollet model for the turbulence of the disperse phase. The only difference is that droplet coalescence is accounted for in the simulation related to figure 8 (right). One observes that the calculation of droplet coalescence results in a higher droplet dispersion in radial direction, especially farther from the nozzle, meeting experimental measurements with a greater agreement. A reason is an increase of the Sauter mean diameter (SMD) due to droplet coalescence, resulting in a lower droplet deceleration. This increase of the SMD is observed in figure 11, where the integral SMD for each measurement location along the spray axis is plotted. Only marginally the same trend is detected for droplet evaporation. In this case, the SMD slightly increases due to the disappearance of small droplets.

In figure 12, simulated and measured local droplet diameter distributions are compared. As expected, the amount of smaller droplets decreases if droplet coalescence is taken into account. Despite the fact that an increase in the amount of larger droplets is not detectable, the measured local NDF is predicted by the DQbSMOM with a satisfactory agreement if droplet coalescence is considered. Also, the plotted curves of simulation results are NDF reconstructions from the calculated quadrature points. These reconstructions are Maximal Entropy approximations based on the moments of the NDF.

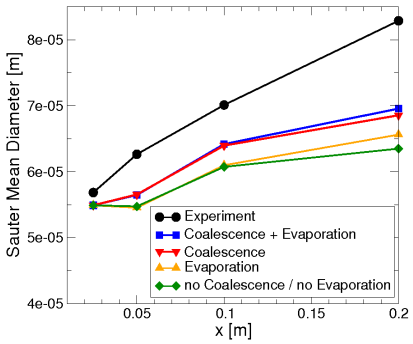

Figure 11. Integral Sauter mean diameter along the spray.

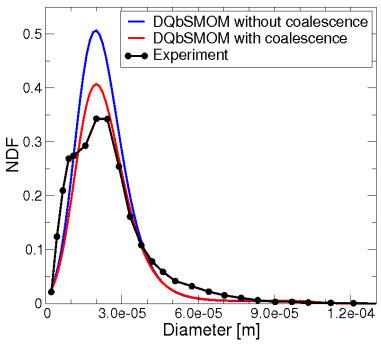

Figure 12. Local droplet diameter distribution at point (x,y) = (50mm, 10mm).

It is also important to mention that a few large droplets are present in the experimental measurements and a high level of statistical noise associated to these droplets is detectable over the inlet profile. For this reason,

these few droplets are neglected such that only 99.98% of the measured droplets are considered for calculating the DQMOM quadrature points, explaining the small deviation between the measured and calculated integral SMD at the inlet location, as seen in figure 11. This is done to achieve more stable simulations and avoid singularities. Note that in a previous publication (see [20]) the authors have considered only about 98% of the measured droplets, which results in a noticeable deviation between the results presented. Also, the divergence of the velocity of the disperse phase has been limited in a few cells of the grid in order to avoid a non-physical accumulation of droplets.

Conclusion

A novel hybrid approach that combines DQMOM with a SM, referred to as the Direct Quadrature based Sectional Method of Moments (DQbSMOM) in this work, has been introduced and a new approach for calculating droplet coalescence, based on the Maximal Entropy approximation of the NDF for integrating the coalescence source terms, has been presented. The EMSM model, considering the d^2-law of evaporation with a constant evaporation rate, has been implemented to calculate the evolution of the NDF due to droplet evaporation. Regarding convective transport and drag, simulation results illustrate the considerably higher accuracy of the DQbSMOM in comparison to the standard DQMOM approach. The droplet coalescence and evaporation phenomena are clearly described by the implemented model and the correct trends are predicted. Two k-ϵ based approaches for modeling the turbulence of the disperse phase have been assessed. Although the standard k-ϵ model for describing the gas phase turbulence along with the Simonin & Viollet model for the turbulence of the disperse phase deliver satisfactory results, weaknesses of this simple modeling have been outlined. Improvement of the turbulence modeling that includes LES is work in progress.

Acknowledgements

The authors would like to thank Professor Marc Massot and his team for their support and the helpful discussions that contributed to this achievement. We also thank the DFG for the financial support.

References

[1] Fox, R. O., Laurent, F., Massot, M., *Journal of Computational Physics* 227:3058-3088 (2008).
[2] Massot, M., Laurent, F., Kah, D., de Chaisemartin, S., *SIAM J. on Applied Mathematics* 70:3203-3234 (2010).
[3] Rüger, M., Hohmann, S., Sommerfeld, M., Kohnen, G., *Atomization and Sprays* 10:47-81 (2000).
[4] Williams, F. A., *Physics of Fluids* 1:541-545 (1958).
[5] Riber, E., Moureau, V., Garcia, M., Poinsot, T., Simonin, O., *J. of Computational Physics* 228:539-564 (2009).
[6] McGraw, R., *Aerosol Science and Technology* 27:225-265 (1997).
[7] Schneider, L., *A Concise Moment Method for Unsteady Polydisperse Sprays*, Ph.D. Thesis, Technische Universität Darmstadt, 2009.
[8] Marchisio, D. L., Fox, R. O., *Journal of Aerosol Science* 36:43-73 (2005).
[9] Belt, R., Simonin, O., *Proc. ASME FEDSM 2009*, FEDSM2009-78095 (2009).
[10] Choi, D., Schneider, L., Spyrou, N., Sadiki, A., Janicka, J., *Proc. 7th International Conference on Multiphase Flow*, Tampa, Florida, May 30 - June 4, 2010.
[11] Friedrich, M., Weigand, B., *Proc. 10th International Conference on Liquid Atomization and Spray Systems*, Kyoto, Japan, August 27 - September 1, 2006.
[12] Madsen, J., Hjertager, B. H., Solberg, T., Norskov, P., Rusas, J., *Proc. 10th International Conference on Liquid Atomization and Spray Systems*, Kyoto, Japan, August 27 - September 1, 2006.
[13] Madsen, J., *Computational and Experimental Study of Sprays from the Breakup of Water Sheets*, Ph.D. Thesis, Esbjerg Institute of Technology, 2006.
[14] Vié, A., Laurent, F., Massot, M., *preprint submitted to Journal of Computational Physics* (2011).
[15] Simonin, O., Viollet, P. L., *Proc. Numerical Methods for Multiphase Flows*, ASME FED 91:73-82 (1990).
[16] Hill, D. P., *The Computer Simulation of Dispersed Two-Phase Flows*, Ph.D. Thesis, Univ. of London, 1998.
[17] Politis, S., *Prediction of Two-Phase Solid-Liquid Turbulent Flow in Stirred Vessels*, Ph.D. Thesis, University of London, 1989.
[18] Kah, D., *Prise en compte des aspects polydispersés pour la modélisation d'un jet de carburant dans les moteurs à combustion interne*, Ph.D. Thesis, École Centrale Paris, 2010.
[19] Mead, L. R., Papanicolaou, N., *Journal of Mathematical Physics* 25:2404-2417 (1984).
[20] Gumprich, W., Sadiki, A., Sommerfeld, M., *Proc. in Applied Mathematics and Mechanics* 11:599-600 (2011).
[21] Gordon, R., *Journal of Mathematical Physics* 9:655-663 (1968).
[22] Sadiki, A., Ahmadi, W., Chrigui, M., Janicka, J., *ERCOFTAC Series* 17:69-110 (2011).
[23] Berlemont, A., Grancher, M. S., Gouesbet, G., *Int. J. of Heat and Mass Transfer* 38:3023-3034 (1995).